Proceedings of "Applications of Physics in Mechanical and Material Engineering" (APMME 2024)

The Influence of the Phase Shift of the Effective Density Vibrations of Layers on the Wave Propagation in Quasi-One-Dimensional Binary Phononic Crystals

S. Garus*

Department of Mechanics and Fundamentals of Machinery Design, Faculty of Mechanical Engineering, Czestochowa University of Technology, Dąbrowskiego 73, 42-201 Częstochowa, Poland

Doi: 10.12693/APhysPolA.147.151 *e-mail: sebastian.garus@pcz.pl

Modern smart materials allow for controlling their properties through external factors such as magnetic, electric, or pressure fields. Using these materials, it is possible to make dynamic phononic crystals with time-varying material parameters. A sinusoidal signal propagating in a static material at the boundary of the media with a dynamic material changes its character to a wave spectrum. Each boundary of the media broadens the spectrum of the propagating wave. These phenomena significantly affect the propagation of a mechanical wave in dynamic phononic crystals by changing the distribution of band gaps. By influencing the frequency and phase shifts of changes in material properties, it is possible to control the operation of phononic crystals, which may allow for the design of new types of smart phononic devices.

topics: mechanical wave, finite-difference time-domain (FDTD), propagation, multilayer

1. Introduction

The structures in which the length of the propagating mechanical wave is comparable to the size of the elements occurring in it are called phononic crystals. Due to their unique properties, they can be used to make devices such as mechanical wave filters [1–4], acoustic barriers [5], acoustic diodes [6], sensors [7], or waveguides [8, 9].

Newly developed materials, the parameters of which can be changed in time, allow for the development of a new class of phononic structures with controlled properties.

Multilayer structures can be built from piezoceramic fibers embedded in epoxy resin and covered with electrodes [10, 11], electroactive polymers (EAP) [12, 13], magnetostrictive composites [14, 15], carbon nanotubes [16], or ferroelectric shape memory alloys [17]. The change in material parameters for the application in phononic crystals has been presented in [18–20]. A time-varying Bragg reflector has been presented in [21, 22].

One of the algorithms in which time-varying material parameters can be directly implemented is the finite-difference time-domain (FDTD) algorithm [23, 24].

The paper analyzes the propagation of a mechanical wave through a single layer of a material with time-varying material parameters and then through a multilayer binary structure. The influence of the phase shift between the wave source and the function describing the change in material parameters was investigated.

2. Research

In this work, the finite-difference time-domain (FDTD) algorithm was used, in which the alternate solving of differential equations

$$\frac{\partial P}{\partial t} = -Z\, c\, \nabla \cdot \boldsymbol{v} \tag{1}$$

and

$$\frac{Z}{c}\frac{\partial \boldsymbol{v}}{\partial t} = -\nabla P \tag{2}$$

allows for the emulation of mechanical wave propagation in the medium.

The properties of the medium are determined by the acoustic impedance Z, and c is the velocity of acoustic wave propagation. In (1)–(2), P is the pressure deviation from the mean value, and $\boldsymbol{v}$

TABLE I

The basic material parameters used for the static phononic structure for layer A (water) [25] and for layer B ($Zr_{55}Cu_{30}Ni_5Al_{10}$) [26].

Layer	c_0 $\left[\frac{\mathrm{m}}{\mathrm{s}}\right]$	ρ_0 $\left[\frac{\mathrm{kg}}{\mathrm{m}^3}\right]$	$Z_0 \times 10^6$ $\left[\frac{\mathrm{kg}}{\mathrm{sm}^2}\right]$
A (water)	1480	1000	1.49
B ($Zr_{55}Cu_{30}Ni_5Al_{10}$)	1633	6829	11.15

determines the velocity of a particle of the medium caused by the instantaneous local pressure difference.

Transforming formulas (1) and (2) into the one-dimensional Euclidean space takes the form

$$\frac{\partial P}{\partial t} = -Z\,c\,\frac{\partial v}{\partial x}, \tag{3}$$

$$\frac{Z}{c}\frac{\partial v}{\partial t} = -\frac{\partial P}{\partial x}. \tag{4}$$

Equations (3) and (4) after discretization and taking into account the time-varying material properties in the FDTD method formalism are defined as

$$P|_x^{n+\frac{1}{2}} = P|_x^{n-\frac{1}{2}} - \frac{Z|_x^{n+\frac{1}{2}}\; c|_x^{n+\frac{1}{2}}\;\Delta t}{\Delta x} \times \left(v|_{x+\frac{1}{2}}^{n} - v|_{x-\frac{1}{2}}^{n}\right), \tag{5}$$

$$v|_{x+\frac{1}{2}}^{n+1} = v|_{x+\frac{1}{2}}^{n} - \frac{Z|_{x+\frac{1}{2}}^{n+1}\;\Delta t}{c|_{x+\frac{1}{2}}^{n+1}\;\Delta x}\left(P|_x^{n+\frac{1}{2}} - P|_{x-1}^{n+\frac{1}{2}}\right). \tag{6}$$

The notation $a|_x^n$ denotes the value of the physical quantity a at point x of space and time step n, where $t = \Delta t\, n$ is assumed as the discretization of time. It should be noted that (5) and (6) are spaced apart by half a time step, and the values of the instantaneous velocity v are located halfway between the pressure nodes P in the grid.

In order to maintain the stability of the simulation, the time step Δt and spatial step Δx values are related to the highest velocity value in the simulation $c_{\max}$ by the Courant condition through

$$\Delta t = \frac{1}{c_{\max}\Delta x}. \tag{7}$$

The analyzed region was surrounded by perfectly matched layers (PML) to suppress waves propagating outside the simulation region.

Layer B was composed of a material for which the basic parameters corresponded to the material parameters for the amorphous compound $Zr_{55}Cu_{30}Ni_5Al_{10}$ presented in Table I (see also [25, 26]) and their variability over time was described by the dependencies

$$Z_B|_x^n = Z_{0,B} + d\,Z_{0,B}\,\sin(2\pi\, m\, f_s\, n\,\Delta t + \varphi), \tag{8}$$

$$c_B|_x^n = c_{0,B} + d\,c_{0,B}\,\sin(2\pi\, m\, f_s\, n\,\Delta t + \varphi), \tag{9}$$

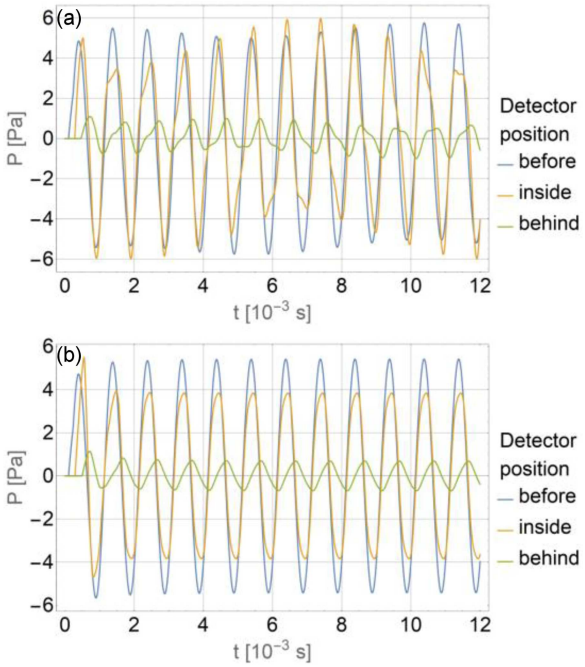

Fig. 1. Pressure time series for the single-layer case: (a) $m = 1.1$, (b) $m = 2$.

where $Z_{0,B}$ and $c_{0,B}$ are the basic acoustic impedance and the sound propagation velocity for material B, respectively, d corresponds to the percentage of change in the amplitude of fluctuations of material values of material B and is 10%, m is the ratio of the frequency of material changes to the source frequency, and φ is the phase shift. Material A was water, and its parameters did not change over time. The materials were selected so that the difference in their acoustic impedance was large.

First, the case of a single layer B with time-varying material parameters surrounded by water was analyzed. The layer thickness was 0.40825 m, the spatial step was $\Delta x = 0.002$ m, and the time step was $\Delta t = 4 \times 10^{-7}$ s. The source of the wave with a frequency of 1000 Hz was 0.232 m away from the layer. In the work, time series of pressure were recorded at three points (detectors) placed respectively 0.1 m before the layer, 0.1 m behind the layer, and inside the layer. The recorded time series for a single layer are shown in Fig. 1 for two different frequencies of changes in material parameters. The corresponding spectra are shown in Fig. 2.

A propagating wave hitting the boundary of the media is partially reflected from it, interfering with the incident wave. Inside the material, part of the wave undergoes multiple reflections between the boundaries of the media. Material parameters that change over time affect the propagating wave. As can be seen in the presented time series, in the case of twice the frequency of changes in material parameters (Fig. 1b), waves with a constant

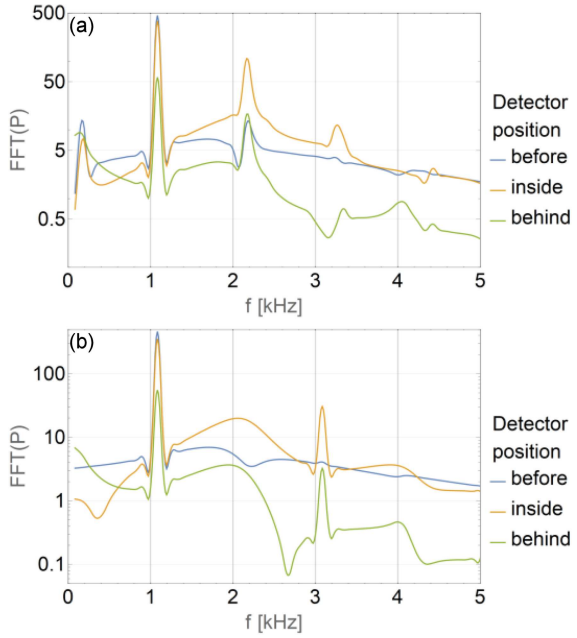

Fig. 2. Waveform spectra for the single-layer case: (a) $m = 1.1$, (b) $m = 2$.

amplitude were created inside and outside the material. On the other hand, in the case shown in Fig. 1b, where the frequency of changes in material parameters was close to the frequency of the wave source, periodic changes in amplitude were observed, i.e., the creation of a low-frequency wave component was observed in the light in Fig. 2a. In both cases, additional peaks related to periodic changes in material parameters were observed in the spectra.

Figure 3 shows how the phase shift between the signal from the wave source and changes in the material parameters of layer B affects the spectrum at the three analyzed points. The phase shift had the greatest effect on the wave inside the layer for the spectral ranges in the spaces between the peaks. However, it did not affect the peaks associated with the wave source, occurring as a result of changes in the material parameter values over time. The range of changes in the spectrum value from the phase shift did not exceed a tenth of the maximum value of the spectrum.

The next stage was to investigate the effect of the phase shift on the ranges of values in the mechanical wave spectrum. The four-layer ABABABABA structure was investigated. The thickness of layer B corresponded to the thickness of the analyzed single-layer case and was selected so that the wave was extinguished in the structure. Figure 4 shows the ranges of the mechanical wave spectrum values inside the successive layers of the structure. The maximum values of the spectrum are marked in blue when the phase shift changes in the range from 0 to 180 degrees, the minimum values are marked in

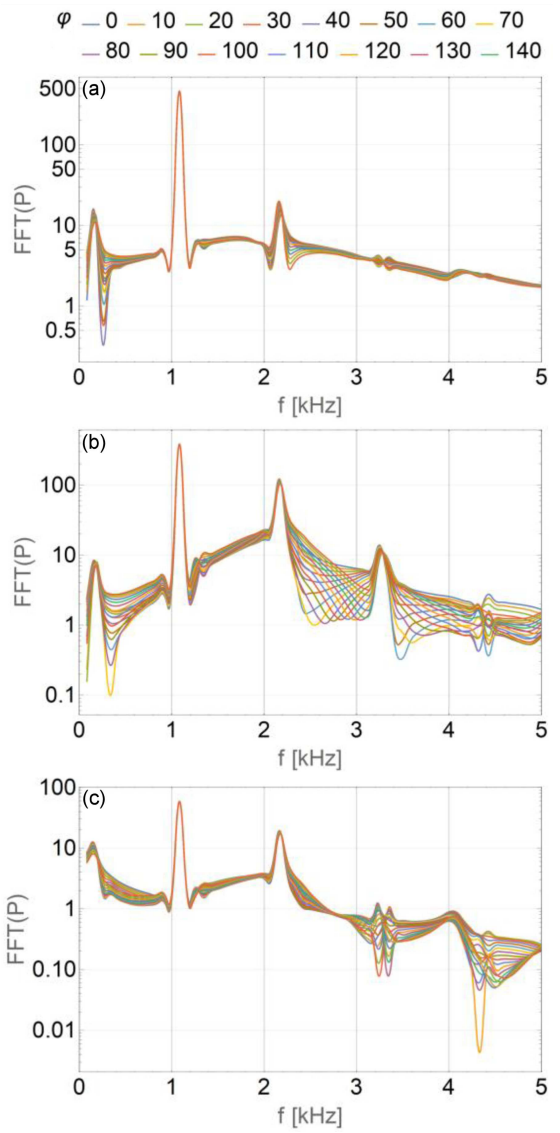

Fig. 3. Influence of the phase shift between the wave source and the changes in material parameters of layer B for the single-layer case with $m = 1.1$: (a) before, (b) inside, (c) behind.

orange, and the area between these values contains intermediate values of the spectrum. Figure 5 shows the influence of the change in the phase shift between the mechanical wave source and the changes in the material parameters of layer B before and behind the analyzed structure.

As can be seen in Fig. 4, the peak associated with the mechanical wave source in each subsequent layer takes on lower values. This is related to the thickness of layer B and the occurrence of a band gap in the source frequency range for the analyzed structure. The peak associated with changes in the values of material parameters occurring at a frequency of 2.1 kHz occurred in all layers, of which its value was similar in the first two, and only in the subsequent layers did the value decrease.

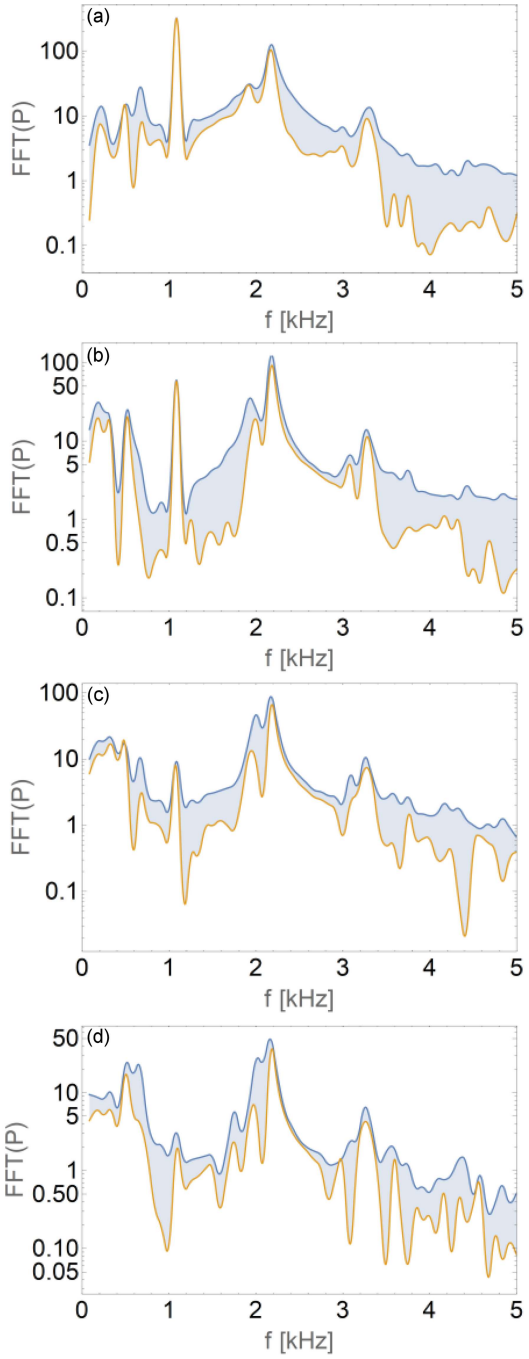

Fig. 4. The influence of phase shift on the ranges of spectral values in subsequent layers of the structure: (a) layer 1, (b) layer 2, (c) layer 3, (d) layer 4.

The greatest influence of the phase shift on the spectrum of the mechanical wave propagating in the structure was observed in the first layer of the structure. Standing waves generated inside the B layers, the proximity of the wave source, the design of the structure so that the mechanical wave does not propagate in it, and multiple reflections inside the structure affect the extension of the range of spectrum values. As can be seen, the greatest ranges

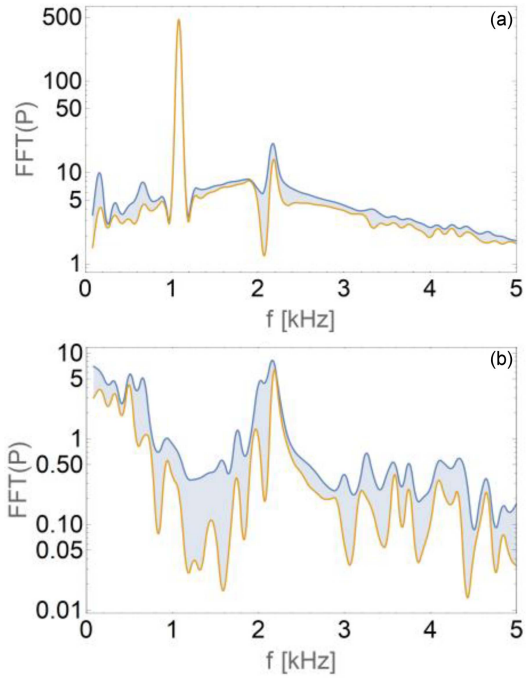

Fig. 5. Influence of phase shift on the ranges of spectral values: (a) before and (b) behind the structure.

of changes in the spectrum values associated with the analyzed influence of the phase shift occur in the spaces between the peaks. In the spectrum of the wave behind the structure (Fig. 5b), there is no peak associated with the wave source because it was reflected from the structure, which can be observed in Fig. 5a.

3. Conclusions

The analysis carried out showed that the use of a material with time-varying material parameters in the phononic structure causes the sine wave propagating in the structure to change its character to a certain range of the spectrum. The phenomenon is intensified when the source and material frequencies are similar.

The phase shift between the wave source and changes in material parameters affects the spectrum distribution, especially in the frequency ranges between high-intensity peaks.

The occurrence of peaks associated with changes in material parameters was demonstrated.

The analyzed phase shift has a negligible effect on the values of the peaks associated with the source and with material changes.

With the increase in the number of layers in the multilayer structure, the intensity of the peak associated with the source decreases faster than with changes in material parameters.

References

[1] W. Sochacki, *Acta Phys. Pol. A* **138**, 328 (2020).

[2] S. Villa-Arango, R. Torres, P.A. Kyriacou, R. Lucklum, *Measurement* **102**, 20 (2017).

[3] C.J. Rupp, M.L. Dunn, K. Maute, *Appl. Phys. Lett.* **96**, 111902 (2010).

[4] S. Garus, W. Sochacki, *Wave Motion* **98**, 102645 (2020).

[5] J.V. Sanchez-Perez, C. Rubio, R. Martinez-Sala, R. Sanchez-Grandia, V. Gomez, *Appl. Phys. Lett.* **81**, 5240 (2002).

[6] X.-F. Li, X. Ni, L. Feng, M.-H. Lu, C. He, Y.-F. Chen, *Phys. Rev. Lett.* **106**, 084301 (2011).

[7] S. Garus, *Rev. Chim.* **70**, 3671 (2019).

[8] J. Wen, D. Yu, L. Cai, X. Wen, *J. Phys. D Appl. Phys.* **42**, 115417 (2009).

[9] B. Morvan, A. Tinel, J.O. Vasseur, R. Sainidou, P. Rembert, A.-C. Hladky-Hennion, N. Swinteck, P.A. Deymier, *J. Appl. Phys.* **116**, 214901 (2014).

[10] M. Melnykowycz, X. Kornmann, C. Huber, M. Barbezat, A.J. Brunner, *Smart Mater. Struct.* **15**, 204 (2006).

[11] R. Paradies, P. Ciresa, *Smart Mater. Struct.* **18**, 035010 (2009).

[12] W.-P. Yang L.-W. Chen, *Smart Mater Struct* **17**, 015011 (2008).

[13] J.-S. Plante, S. Dubowsky, *Smart Mater. Struct.* **16**, 227 (2007).

[14] S. Levgold, J. Alstad, J. Rhyne, *Phys. Rev. Lett.* **10**, 509 (1963).

[15] C. Rodríguez, M. Rodriguez, I. Orue, J.L. Vilas, J.M. Barandiarán, M.L.F. Gubieda, L.M. Leon, *Sens. Actuators A* **149**, 251 (2009).

[16] A.E. Aliev, J. Oh, M.E. Kozlov, A.A. Kuznetsov et al., *Science* **323**, 1575 (2009).

[17] Y. Ganora, D. Shilo, J. Messier, T.W. Shield, R.D. James, *Rev. Sci. Instrum.* **78**, 073907 (2007).

[18] D.W. Wright, R.S.C. Cobbold, *Smart Mater. Struct.* **18**, 015008 (2009).

[19] E.S. Cassedy, *Proc. IEEE* **55**, 1154 (1967).

[20] C. Elachi, *IEEE Trans. Antennas Propag.* **20**, 534 (1972).

[21] J.H. Wu, T.H. Cheng, A.Q. Liu, *Appl. Phys. Lett.* **89**, 263103 (2006).

[22] A. Kupczyk, J. Świerczek, M. Hasiak, K. Prusik, J. Zbroszczyk, P. Gębara, *J. Alloys Compd.* **735**, 253 (2018).

[23] Y. Tanaka, Y. Tomoyasu, S.-I. Tamura, *Phys. Rev. B* **62**, 7387 (2000).

[24] X. Liu, D.A. McNamara, *Int. J. Infrared Milli. Waves* **28**, 759 (2007).

[25] Y. Wang, W. Song, E. Sun, R. Zhang, W. Cao, *Physica E* **60**, 37 (2014).

[26] S. Garus, M. Bold, W. Sochacki, *Acta Phys. Pol. A* **135**, 139 (2019).